DOI 10.5012/bkcs.2010.31.5.1295

# Kinetic Investigation of $CO_2$ Reforming of $CH_4$ over Ni Catalyst Deposited on Silicon Wafer Using Photoacoustic Spectroscopy

**Jin-Hyuck Yang, Ji-Woong Kim, Young-Gil Cho,[†] Hong-Lyoul Ju,[‡] Sung-Han Lee,[†,*] and Joong-Gill Choi[*]**

*Department of Chemistry, Yonsei University, Seoul 120-749, Korea. [*]E-mail: jgchoi@yonsei.ac.kr*
*[†]Department of Chemistry, Yonsei University, Wonju 220-710, Korea. [*]E-mail: shl2238@yonsei.ac.kr*
*[‡]Department of Physics, Yonsei University, Seoul 120-749, Korea*
*Received January 20, 2010, Accepted March 12, 2010*

The $CO_2$-$CH_4$ reaction catalyzed by Ni/silicon wafers was kinetically studied by using a photoacoustic technique. The catalytic reaction was performed at various partial pressures of $CO_2$ and $CH_4$ (50 Torr total pressure of $CO_2/CH_4/N_2$) in the temperature range of 500 - 650 °C in a static reactor system. The photoacoustic signal that varied with the $CO_2$ concentration during the catalytic reaction was recorded as a function of time. Under the reaction conditions, the $CO_2$ photoacoustic measurements showed the as-prepared Ni thin film sample to be inactive for the reaction, while the $CO_2/CH_4$ reactions carried out in the presence of the sample pre-treated in $H_2$ at 600 °C were associated with significant time-dependent changes in the $CO_2$ photoacoustic signal. The rate of $CO_2$ disappearance was measured from the $CO_2$ photoacoustic signal data in the early reaction period of 50 - 150 sec to obtain precise kinetic data. The apparent activation energy for $CO_2$ consumption was determined to be 6.9 kcal/mol from the $CO_2$ disappearance rates. The partial reaction orders, determined from the $CO_2$ disappearance rates measured at various $P_{CO_2}$'s and $P_{CH_4}$'s at 600 °C, were determined to be 0.33 for $CH_4$ and 0.63 for $CO_2$, respectively. Kinetic data obtained in these measurements were compared with previous works and were discussed to construct a catalytic reaction mechanism for the $CO_2$-$CH_4$ reaction over Ni/silicon wafer at low pressures.

**Key Words**: Ni/silicon wafer catalyst, $CO_2$ reforming of $CH_4$, Photoacoustic spectroscopy

## Introduction

The $CO_2$ reforming reaction of $CH_4$ can be utilized to make a synthesis gas with a low $H_2/CO$ ratio that is suitable for the production of oxygenated chemicals, such as aldehydes, methyl alcohol, and acetic acid. A nickel catalyst is proved to be effective for the reaction, but it is easily deactivated by carbon deposition on the surface during the reaction. The coking tendency of a nickel catalyst largely depends on the type of a support so that many supported Ni catalysts have been studied in the context of the $CO_2$ reforming reaction of $CH_4$. However, these studies have been mainly focused on the development of coking-resistant catalysts and little kinetic investigation has been performed for the Ni-catalyzed $CO_2$-$CH_4$ reaction.[1] Accordingly, there still exists a controversy to assign a detailed mechanism for this important reaction.

The researches on the catalytic activity of the reactions involve the quantitative studies of reaction rate. For the kinetic experiments, thereby, it is desirable to measure the concentrations of reactants and/or products of interest as a function of time so that an inflection point or a short induction period can be clearly observed from the kinetic curves. Although absorption spectroscopic techniques are generally employed to the direct measurement of concentrations, their sensitivities may be diminished due to the difficulty in the observation of differences between the incident and transmitted intensities of radiation. Moreover, these techniques have often limited success in measuring temporal changes precisely in the concentrations at short reaction times where the rates are large. In contrast, the photoacoustic spectroscopic (PAS) technique measures the acoustic waves generated from the absorption of optical energy directly, avoiding these limitations. Note also that its highly selective detection and extremely low molecular gas level detection limit can provide an acoustic signal with enough intensity for even time-resolved experiments.[2,3] In addition, a further advantage of this technique is to measure the concentrations of analytes without utilizing any sophisticated sampling techniques which are inevitable in the conventional techniques such as gas chromatography or mass spectroscopy. Since the PAS technique can directly measure the absorption characteristics of the samples of interest with possessing inherent high sensitivity and practical advantages, the technique is considered to be suitable for *in situ* monitoring of the catalytic reactions. In the previous reports,[3-7] we have demonstrated that the PAS technique can be utilized to obtain the precise kinetic data of the catalytic reactions in which $CO_2$ is involved as reactants or products.

As mentioned earlier the most consideration of previous studies of Ni-catalyzed $CO_2$-$CH_4$ reaction has been related to the development of coking-resistant nickel catalysts and kinetic data available for these reactions have been mostly obtained for metal oxide-supported catalysts. Moreover, little kinetic data have been obtained for the reaction process[1] and those reported have been determined for the most part by monitoring the rates of $CH_4$ consumption.[8,9] In this work, a kinetic study of the catalytic $CO_2$-$CH_4$ reaction was performed by measuring the rates of $CO_2$ consumption by the use of a thin Ni metal deposited on silicon wafer which has not been yet examined as a catalyst for the $CO_2$-$CH_4$ reaction. The temporal variations of $CO_2$ concentration during the reaction were monitored by *in situ* PAS and a suitable differential photoacoustic cell in the temperature range of 500 - 650 °C. The apparent activation energy and reaction orders were calculated by the photoacoustic data determined from the

rates of $CO_2$ disappearance in the early reaction stage. The kinetic results obtained in these experiments were discussed and compared with those of previous works to infer a mechanism for the Ni-catalyzed $CO_2$-$CH_4$ reaction at low pressures.

## Experimental

A nickel thin film deposited on silicon (100) wafer substrate with a native oxide layer was prepared by a DC-magnetron sputtering system from a Ni target (99.99% purity Ni disc of 5.1 cm in diameter). The chamber was evacuated at a pressure of $5 \times 10^{-6}$ Torr or below before the deposition. During deposition, the deposition pressure in the chamber was $5 \times 10^{-3}$ Torr in flowing argon (99.99% purity) gas with a flow rate of 50 $cm^3$/min and the sputtering power was 50 W. FE-SEM (field emission-scanning electron microscopy) images of samples were obtained with a Hitachi SU70. An X-ray diffraction (XRD) analysis of samples was performed at room temperature by using a Philips PW-1710 diffractometer with Cu-Kα radiation.

The details of the experimental arrangement for the PAS detection to monitor the catalytic reactions are described in previous papers.[3,4] Photoacoustic measurements were performed by using a differential photoacoustic cell consisted of two compartments, i.e. a reference cell and a sample cell, separated from each other by a ZnSe window. Each photoacoustic cell was a Helmholtz resonator of 1.9 cm in diameter and 3.3 cm in length with an adjoining tube of 1.0 cm in diameter and 10 cm in length. The output beam of a cw $CO_2$ laser (Synrad Series 48-1-28) operating in multiline of 10.6 μm was modulated at 25 Hz. The nonresonant condition was used in order to prevent the change of the signal due to the variation in the resonance frequency followed by the temperature change in the Helmholtz resonator. The photoacoustic signals detected by the microphones in the sample (signal A) and reference (signal B) cell were amplified by a lock-in amplifier (EG & G Princeton Applied Research Model 5210) and the signal ratio (A/B) was recorded by a personal computer as a function of time.

The sensitivity of the photoacoustic signal generally increases with decreasing the total pressure of gas medium. Hence, the total pressure of gaseous reactants in the reactor was kept at 50 Torr filled with $N_2$ as a buffer gas in these measurements. The reference cell was filled with a gaseous mixture of $CO_2$ (0.2 Torr) and $N_2$ (49.8 Torr) to obtain the signal B. The sample cell was directly connected to a quartz microreactor with 21 $cm^3$ volume approximately 15 cm away by an adjoining tube. The fragment of Ni thin film with a size of 10 mm × 10 mm was used as catalyst for the reaction. The catalyst loaded in the reactor was typically treated in a flow of $H_2$ at 600 °C for 1 h prior to each kinetic measurement. After the pre-treatment of the catalyst, the reactor was cooled down to room temperature and helium gas was passed to remove hydrogen gas remaining in the microreactor. The reaction mixture containing methane and carbon dioxide was then admitted into the microreactor at a given temperature in the range of 500 - 650 °C. The purity of $CH_4$, $CO_2$, and $N_2$ gas was greater than 99.99%. The gas pressure was monitored with a capillary silicon oil manometer (1/13 Torr precision) and a pirani gauge.

## Results

It is noted that the PAS technique is applicable to the quantitative analysis by monitoring the progress of reactions, since the photoacoustic signal is directly proportional to the concentration of analyte in a given condition. The experiments in this work were performed in the linear response range of the $CO_2$ photoacoustic signal with respect to the $CO_2$ partial pressure of below 10 Torr and the power of the incident laser beam of less than 8 W. A blank test, performed using $CO_2$/$CH_4$/$N_2$ (8 Torr/8 Torr/34 Torr) mixture in the absence of catalyst, showed no variation of the $CO_2$ photoacoustic signal in the temperature range of 500 - 650 °C. It was also found that the silicon wafer itself used as a substrate in this work was not active for the reaction.

Fig. 1 shows the surface morphology and the cross section SEM images of the as-prepared sample. The Ni thin film with a thickness of ~60 nm was composed of the small crystalline particles which were uniformly distributed all over the surface of the substrate. Fig. 2 exhibits the XRD pattern of the as-prepared Ni film. The XRD peak located at 39.2° corresponds to the (010) planes of hexagonal Ni metal and the other small peaks are at-

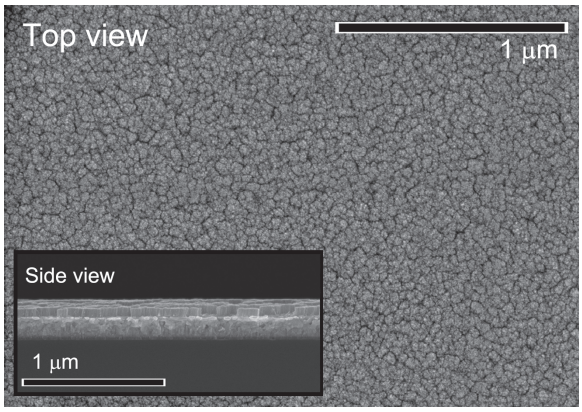


**Figure 1.** SEM images of Ni thin film deposited on silicon wafer.

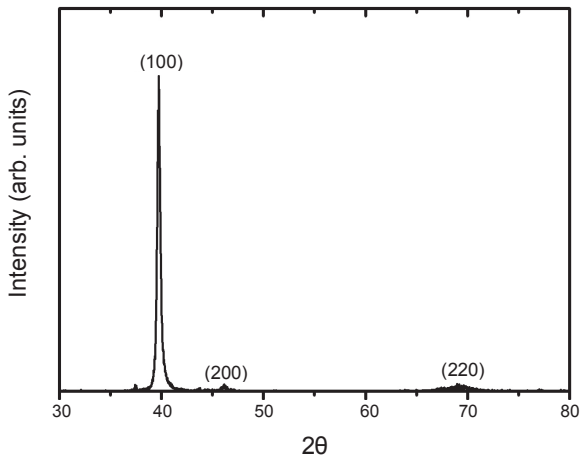


**Figure 2.** X-ray diffraction pattern of Ni thin film deposited on silicon wafer. Ni (JCPDS no. 45-1027); NiOOH (JCPDS no. 27-0956).

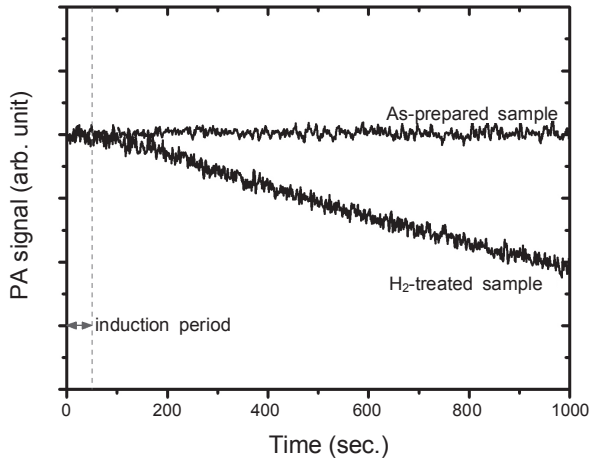


**Figure 3.** $CO_2$ photoacoustic signals for $CO_2$-$CH_4$ reaction as a function of time at 500 °C on as-prepared Ni/silicon wafer and $H_2$-treated Ni/silicon wafer; $CO_2$(g)/ $CH_4$(g)/$N_2$(g) (8/8/34 in Torr) reaction mixture.

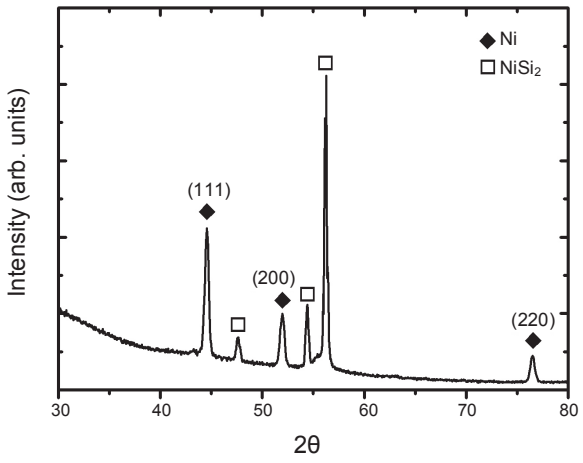


**Figure 5.** X-ray diffraction pattern of Ni/silicon wafer treated in $H_2$ at 600 °C for 1 h. Ni(JCPDS no. 04-0850); NiOOH(JCPDS no. 27-0956); Nickel silicide(JCPDS no. 41-0775).

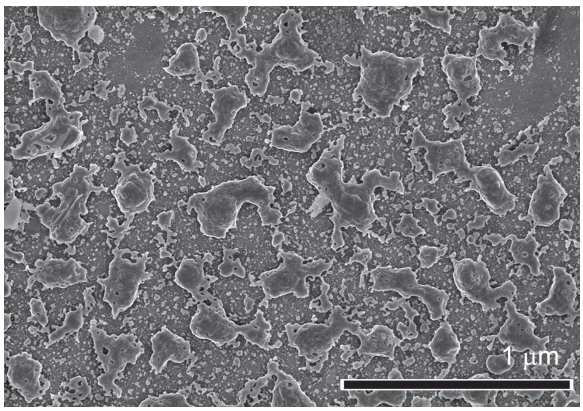


**Figure 4.** SEM image of Ni/silicon wafer treated in $H_2$ at 600 °C for 1 h.

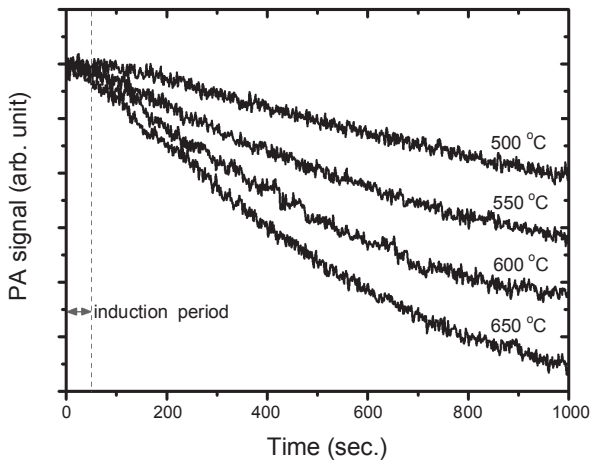


**Figure 6.** Variations of $CO_2$ photoacoustic signal with time at various temperatures for $CO_2$-$CH_4$ reaction over $H_2$-treated Ni/silicon wafer; $CO_2$(g)/$CH_4$(g)/$N_2$(g) (8/8/34 in Torr) reaction mixture.

tributed to nickel oxyhydroxide which is formed during the exposure to air prior to the XRD analysis.

In Fig. 3 is displayed the variations of the $CO_2$ photoacoustic signal with time for the $CO_2$-$CH_4$ reaction at 500 °C over both the as-prepared sample and the sample treated in $H_2$ for 1 h. The reaction over the as-prepared sample reveals a very slight decrease in the $CO_2$ photoacoustic signal, while the reaction over the $H_2$-treated sample demonstrates a significant decrease in the signal. It is also observable that the $CO_2$ photoacoustic curve for the $H_2$-treated sample shows to have an initial induction period. The SEM and XRD results of the $H_2$-treated sample are shown in Figs. 4 and 5, respectively. The SEM result shows that the Ni film structure is broken during the pre-treatment. The XRD pattern exhibits the (111) preferential plane of cubic Ni metal, in which nickel oxyhydroxide and nickel silicides are observed as XRD detectable phases. The XRD result also indicates that Ni metal structure is changed from hexagonal to cubic during the pre-treatment.

The effect of temperature on the $CO_2$ disappearance rate for the $CO_2$-$CH_4$ reaction over the $H_2$-treated catalyst was investigated in the temperature range of 500 - 650 °C. Fig. 6 shows the variations of the $CO_2$ photoacoustic signal with time at various temperatures, exhibiting the presence of initial induction period in each curve. The rates of $CO_2$ disappearance were determined from the slope of curves in the period of 50 - 150 sec. The rates were then plotted as a function of reciprocal temperature according to the Arrhenius equation, as shown in Fig. 7. The apparent activation energy from the Arrhenius plot was calculated to be 6.9 kcal/mol. The $P_{CO_2}$ and $P_{CH_4}$ dependences of the $CO_2$ disappearance rate were measured at various partial pressures of $CO_2$ and $CH_4$. The reaction orders were then determined from the best fit of the rate data for $CO_2$ consumption to the power rate law, $rate = kP_{CO_2}^{\alpha}P_{CH_4}^{\beta}$. Fig. 8 shows the $P_{CO_2}$ and $P_{CH_4}$ dependences of the $CO_2$ consumption rate for the $CH_4$-$CO_2$ reaction on the $H_2$-treated catalyst. The reaction orders determined from the slopes of curves were 0.63 with respect to $CO_2$ and 0.33 with respect to $CH_4$. In Fig. 9 is displayed the XRD pattern of the used catalyst, in which nickel oxide and nickel oxyhydroxide are observed as XRD detectable phases. The result indicates that nickel catalyst has been oxidized in part during the catalytic reaction.

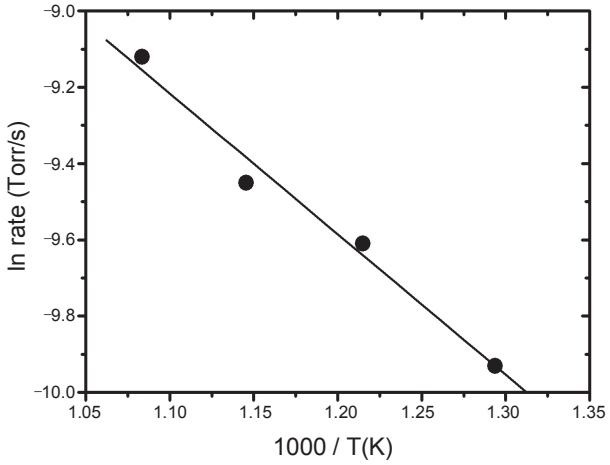


**Figure 7.** Rate of $CO_2$ disappearance *vs*. 1/T for $CO_2$-$CH_4$ reaction over $H_2$-treated Ni/silicon wafer.

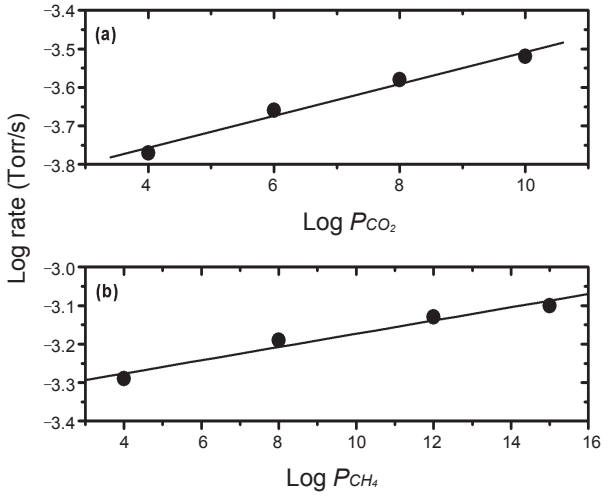


**Figure 8.** (A) $P_{CO_2}$ dependence and (B) $P_{CH_4}$ dependence of $CO_2$ disappearance rate for $CO_2$-$CH_4$ reaction over $H_2$-treated Ni/silicon wafer at 600 °C.

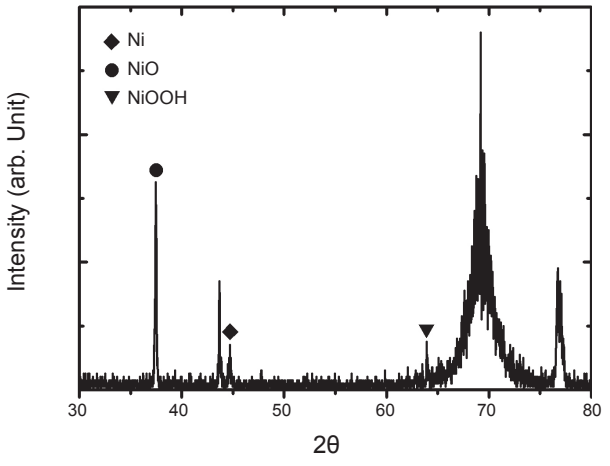


**Figure 9.** X-ray diffraction pattern of $H_2$-treated Ni/silicon wafer after catalytic $CO_2$-$CH_4$ reaction. Ni (JCPDS no. 04-0850); NiOOH (JCPDS no. 27-0956); NiO (JCPDS no. 47-0850).

## Discussion

As shown in Fig. 3, the $H_2$-treated Ni/silicon wafer appreciably promoted a change in the $CO_2$ photoacoustic signal for the $CO_2$-$CH_4$ reaction, while the as-prepared Ni film failed to exhibit a change in the signal, indicating an importance of the $H_2$-treatment on the catalytic activity for the reaction. The XRD pattern of the as-prepared sample showed the (010) preferential plane of hexagonal Ni and that of the $H_2$-treated sample showed the (111) preferential plane of cubic Ni, as revealed in Figs. 2 and 4. It is considered from the results that the Ni (111) plane is active for the reaction, but the Ni (010) plane is not active. Since catalytic property of nickel thin film or nickel/silicon wafer for the $CO_2$ reforming of $CH_4$ has not been reported yet, it is not possible to compare directly the present data with others. Moreover, kinetic data reported for the catalytic $CO_2$-$CH_4$ reaction have been determined for the most part by monitoring the rate of $CH_4$ consumption.[8] It is interesting to compare the earlier data with those determined from the rate of $CO_2$ consumption in the $CO_2$-$CH_4$ reaction over Ni catalyst.

According to kinetic data of the Ni-catalyzed $CO_2$-$CH_4$ reaction, the apparent activation energies for $CH_4$ consumption or $CO_2$ consumption vary with the supports used and are in the range of 7 - 28 kcal/mol.[4] Bradford and Vannice[8] determined the apparent activation energy for $CO_2$ consumption to be 19 kcal/mol for the Ni/$SiO_2$-catalyzed $CO_2$-$CH_4$ reaction, which is greater than 6.9 kcal/mol obtained in this work. It is noted that they performed the reaction in a flow reactor at a total pressure of 740 Torr in the temperature range of 400 - 550 °C, while our experiments were carried out in a static reactor at a total pressure of 50 Torr in the temperature range of 500 - 650 °C. Takano *et al*.[9] studied the $CO_2$ reforming of $CH_4$ over Ni/$Al_2O_3$ catalyst at a total pressure of 63 Torr and reported the apparent activation energy for $CH_4$ consumption to be 10.4 kcal/mol. In general, the apparent activation energy determined from the $CH_4$ consumption in the $CO_2$ reforming of $CH_4$ is somewhat higher than that from $CO_2$ consumption. From the consideration, the present value is believed to be in reasonable agreement with theirs.

The reaction orders obtained in present work are also difficult to compare directly with others. In this experiment, the reaction orders were determined to be 0.33 with respect to $CH_4$ and 0.63 with respect to $CO_2$. In our previous studies,[6] the reaction orders determined from the rate of $CO_2$ disappearance in the $CO_2$-$CH_4$ reaction over Ni/$SiO_2$ catalyst at a total pressure of 40 Torr have been found to be 0.32 and 0.65 with respect to $CH_4$ and $CO_2$, respectively, which are nearly equal to those of current work. Bradford and Vannice[8] also reported very similar results to our values such that the reaction orders determined from the $CO_2$ consumption rate were 0.27 with respect to $CH_4$ and 0.64 with respect to $CO_2$.

As described early, catalytic properties of Ni catalyst for the $CO_2$-$CH_4$ reaction can be varied with the type of support used. When a reducible metal oxide like $TiO_2$ is applied as a support for Ni catalyst, the support itself participates the catalytic $CO_2$-$CH_4$ reaction, in which oxygen vacancies formed during the pre-reduction can act as active sites for dissociative adsorption of $CO_2$.[8,10] On the other hand, when an irreducible oxide support like silica is used, the $CO_2$ dissociation is promoted by the H

(ads) originating from the $CH_4$ dissociation which can be assisted by oxygen atoms on the support.[11] The silicon wafer, used as a support in this work, contains neither oxygen vacancies nor oxygen atoms in it. Additionally, the Ni (111) plane is known to be inactive for the dissociative adsorption of $CO_2$.[12] Thus other process for the $CO_2$ dissociation on the present catalyst must be considered. The Ni (111) plane is not active for the $CO_2$ dissociation,[12] but active for the $CH_4$ dissociation.[13] Hence, the $CH_4$ dissociation is believed to occur prior to the $CO_2$ dissociation over the present catalyst. Although there are some disagreements in the reaction mechanism of catalytic $CO_2$-$CH_4$ reaction, it is generally accepted that methane is dissociatively adsorbed on the surface of the metal catalyst to form both $CH_x$ fragment and H(ads)[1,14]: $CH_4(g) \rightleftharpoons CH_x(ads) + (4\text{-}x)\,H(ads)$. It has been also proved that a reverse water-gas shift reaction, $CO_2(g) + H_2(g) \rightarrow CO(g) + H_2O(g)$, as a side reaction is involved in the reaction mechanism. The reverse water-gas shift reaction can occur in the temperature range of 500 - 650 °C, explored in these measurements, and the reaction on the catalyst surface could be represented as $CO_2(ads) + H(ads) \rightleftharpoons CO(ads) + OH(ads)$, which means that the $CO_2$ dissociation is promoted by the H (ads). The OH (ads) groups are evolved from the surface as $H_2O$ (g) to leave O (ads) on the surface: $2OH(ads) \rightleftharpoons H_2O(g) + O(ads)$.

If the reverse water-gas shift reaction is favorable under these conditions, the rate of $CO_2$ disappearance would increase with increasing temperature in the given region. As a result, the observation of high apparent activation energy for the $CO_2$ consumption is expected. However, the apparent activation energy obtained in this work, 6.9 kcal/mol, is rather low, which enables us to consider that other side reactions may occur in this catalytic reaction. Both the CO disproportionation ($2CO(g) \rightleftharpoons CO_2(g) + C(s)$) and the methane cracking ($CH_4(g) \rightleftharpoons 2H_2(g) + C(s)$) can be considered as side reactions under the reaction conditions. In both the side reactions producing solid carbon, the methane cracking would be more preferable at low pressures. Carbon species formed from the methane cracking, which may be regarded as intermediates in the reaction, are known to have high reactivity.[8,15] When the active carbon species react with water vapor formed in the catalytic reaction, CO, $CO_2$, and $H_2$ can be produced according to the processes: $C(s) + H_2O(g) \rightleftharpoons CO(g) + H_2(g)$ or $C(s) + 2H_2O(g) \rightleftharpoons CO_2(g) + 2H_2(g)$. Note that both the reactions are considered to be favorable at low pressures[3] and the occurrence of the reaction can suppress the deposition of solid carbon on the catalyst surface. The $CO_2(g)$ production from the side reaction would give rise to a little change in the total $CO_2$ photoacoustic signal during the reaction and, accordingly, the low apparent activation energy for the $CO_2$ consumption would be observed.

It is noticeable that the $CO_2$ photoacoustic curves in Fig. 6 reveal an initial induction period. The observation of the initial induction period implies that intermediates may be involved in the reaction mechanism or other active sites may be generated in the early reaction stage. Many mechanistic studies for the $CO_2$ reforming of $CH_4$ over supported Ni and Pt catalysts have been proposed that surface $CH_x$ fragments produced from the dissociative adsorption of $CH_4$ react with either oxygen atoms or hydroxyl groups to form $CH_xO$ intermediates: $CH_x + O \rightleftharpoons CH_xO$, $CH_x + OH \rightleftharpoons CH_xO + H$.[8,16-18] The $CH_xO$ intermediates are subsequently decomposed into both CO and $H_2$ products: $CH_xO(ads) \rightarrow CO(ads) + H_x(g)$. In order to form the $CH_xO$ intermediates, the $CO_2$ dissociation must be occurred prior to the reaction of $CH_x$ fragments, suggesting that the $CO_2$ dissociation depends on the $CH_4$ dissociation into $CH_x$ fragments and H (ads). If $CH_xO$ is an intermediate in the reaction mechanism, the rate of $CO_2$ consumption should be dependent on the partial pressure of methane, as was observed in this study.

As shown in Fig. 9, the XRD pattern of the catalyst after the reaction revealed the presence of nickel oxide and nickel oxyhydroxide phases. The result indicates that Ni metal was oxidized during the catalytic reaction, in which oxygen atoms should be provided from $CO_2$. The reaction of $CO_2(ads)$ with H (ads) generates both CO and OH (ads) and the OH (ads) groups are evolved from the surface such as $H_2O$ to leave O atom on the surface, thereby resulting the oxidation of nickel. It is expected that the reaction of $CH_x$ fragments with either O atoms or OH groups to form $CH_xO$ intermediates can occur favorably in the nickel-nickel oxide interfacial region. When the concentration of $CH_xO$ intermediates rises to a maximum, the $CO_2$ concentration would begin to decrease gradually with increasing the concentrations of CO and $H_2$ products. Consequently, a gradual decrease in the $CO_2$ photoacoustic signal along with time would be observed. The initial induction period, observed in the current work, is considered as the time required to reach the maximum in the concentration of $CH_xO$ intermediate with the formation of nickel oxide.

In this report, the kinetic analysis of the $CO_2$-$CH_4$ reaction catalyzed by nickel metal deposited on silicon wafer was performed at a total pressure of 50 Torr in the temperature range of 500 - 650 °C by using the $CO_2$ laser-based photoacoustic method. An initial induction period was observed from the $CO_2$ photoacoustic curves recorded as a function of time for the catalytic reaction. The observation of initial induction period is considered to be closely related to the formations of nickel oxide and $CH_xO$ intermediates during the reaction. It is also suggested that in the nickel-nickel oxide interfacial regions, the $CH_x$ fragments originated from $CH_4$ react with OH groups or O atoms to form $CH_xO$ intermediates which subsequently decompose into both CO and $H_2$ products. The low apparent activation energy for the $CO_2$ disappearance observed in this work, 6.9 kcal/mol, seems to be resulted from the occurrence of the side reactions between solid carbon and water vapor to produce $CO_2$. It should be pointed out that since these measurements were conducted at low pressures, the kinetic data obtained may be different from those measured at high pressures. Nevertheless, the photoacoustic technique and its capability of low molecular level detection at the early reaction stage enable us to obtain precise and useful kinetic information about the reaction mechanism.

**Acknowledgments.** This work was supported by grant No. 2006-000-10330-0 from the Basic Research Program of the Korea Science & Engineering Foundation and by the Brain Korea 21 Project of the Ministry of Education, Science and Technology of Korea. Authors thanks KBSI Gangneung Center for FE-SEM measurements.

## References


1. Bradford, M. C. J.; Vannice, M. A. *Catal. Rev. Sci. Eng*. **1999**, *41*, 1.
2. Choi, J. G.; Diebold, G. J. *Anal. Chem*. **1987**, *59*, 519.
3. Kim, J. W.; Ha, J. A.; Jung, H.; Ahn, B. I.; Lee, S. H.; Choi, J. G. *Phys. Chem. Chem. Phys*. **2007**, *9*, 5828.
4. Kim, S. J.; Byun, I. S.; Han, H. Y.; Ju, H. L.; Lee, S. H.; Choi, J. G. *Appl. Catal. A*: *Gen*. **2002**, *234*, 35.
5. Byun, I. S.; Choi, O. L.; Choi, J. G.; Lee, S. H. *Bull. Korean Chem. Soc*. **2002**, *23*, 1513.
6. Koh, H. W.; Lee, S. H.; Choi, J. G. *Bull. Korean Chem. Soc*. **2004**, *25*, 1253.
7. Jung, H.; Kim, J. W.; Cho, Y. G.; Jung, J. S.; Lee, S. H.; Choi, J. G. *Appl. Catal. A*: *Gen*. **2009**, *368*, 50.
8. Bradford, M. C. J.; Vannice, M. A. *Appl. Catal. A*: *Gen*. **1996**, *142*, 97.
9. Takano, A.; Tagawa, T.; Goto, S. *J. Chem. Eng. Jpn*. **1994**, *27*, 727.
10. Wang, S.; Lu, G. Q.; Millar, G. J. *Energy Fuels* **1996**, *10*, 896.
11. Erdöhelyi, A.; Csrenyi, J.; Papp, E.; Solymosi, F. *Appl. Catal. A*: *Gen*. **1994**, *108*, 205.
12. Solymosi, F. J. *Mol. Catal*. **1991**, *65*, 337.
13. Beebe, T. P.; Goodman, D. W.; Kay, B. D.; Yates, J. T. *J. Chem. Phys*. **1987**, *87*, 2305.
14. Munera, J. F.; Irusta, S.; Cornaglia, L. M.; Lombardo, E. A.; Cesar, D. V.; Schmal, M. *J. Catal*. **2007**, *245*, 25.
15. Kroll, V. C. H.; Swaan, H. M.; Lacombe, S.; Mirodatos, C. *J. Catal*. **1997**, *164*, 387.
16. Bradford, M. C. J.; Vannice, M. A. *J. Catal*. **1998**, *173*, 157.
17. Chang, J. S.; Park, S. E.; Chon, H. *Appl. Catal. A*: *Gen*. **1996**, *145*, 111.
18. Wang, H. Y.; Au, C. T. *Catal. Lett*. **1996**, *38*, 77.